

Femtosecond nuclear motion of HCl probed by resonant x-ray Raman scattering in the Cl 1s region

M. Simon,^{1,*} L. Journal,¹ R. Guillemin,^{1,2} W. C. Stolte,² I. Minkov,³ F. Gel'mukhanov,^{3,†} P. Sałek,³ H. Ågren,³ S. Carniato,¹ R. Taïeb,¹ A. C. Hudson,² and D. W. Lindle²

¹Laboratoire de Chimie Physique-Matière et Rayonnement, UMR 7614, 11 rue Pierre et Marie Curie, 75231 Paris Cedex 05, France

²Department of Chemistry, University of Nevada, Las Vegas, Nevada 89154, USA

³Theoretical Chemistry, Roslagstullsbacken 15, Royal Institute of Technology, S-106 91 Stockholm, Sweden

(Received 29 June 2005; published 24 February 2006)

Femtosecond dynamics are observed by resonant x-ray Raman scattering (RXS) after excitation along the dissociative Cl $1s \rightarrow 6\sigma^*$ resonance of gas-phase HCl. The short core-hole lifetime results in a complete breakdown of the common nondispersive behavior of soft-x-ray transitions between parallel potentials. We evidence a general phenomenon of RXS in the hard-x-ray region: a complete quenching of vibrational broadening. This opens up a unique opportunity for superhigh resolution x-ray spectroscopy beyond vibrational and lifetime limitations.

DOI: 10.1103/PhysRevA.73.020706

PACS number(s): 33.80.Eh, 34.50.Gb, 33.70.Ca

Time-resolved x-ray spectroscopy is an emerging field with applications as diverse as structural determination of biomolecules in living organisms and dynamics of physical-chemical processes [1]. Many of these applications require both spectral tunability and femtosecond time resolution of the x-ray sources. Unfortunately, current and future synchrotron radiation sources and free-electron x-ray lasers have rather long pulse durations, ≥ 100 fs. The only exceptions are femtosecond UV and soft-x-ray sources in the energy range below 300 eV produced by high-harmonic generation [2], which have been successfully applied to ultrafast pump-probe measurements [2,3]. In contrast, resonant x-ray Raman scattering (RXS) allows the study of ultrafast dynamics and high-energy resolution decay spectra with long-pulse light sources. This uses the concept of an effective duration time of the scattering process to extract temporal dynamics *a posteriori* [4,5].

To date, numerous x-ray studies of ultrafast nuclear dynamics, usually defined as dissociation faster than the core-hole lifetime, have been undertaken in the soft-x-ray region below 1 keV using the nonradiative technique of resonant Auger electron spectroscopy (see available reviews [5–7]). Core-hole lifetimes in this energy range are several femtoseconds long, and ultrafast fragmentation on this time scale has been observed in hydrogen halides, diatomic molecules such as oxygen and nitrogen, and polyatomic molecules such as ozone, water, ammonia, and sulfur hexafluoride [8–11,6,12]. In this energy range, RXS is difficult to measure because radiative decay is very weak. The OCS molecule is an example of ultrafast (~ 10 fs) dissociation studied via radiative soft-x-ray emission [13].

In this paper, we present an observation of femtosecond-scale nuclear dynamics in the hard-x-ray region (>1 keV). Here, the well-known disadvantage of hard-x-ray spectroscopy,

namely large lifetime broadening, becomes an advantage in the time domain because of the shortening of the time scale (~ 1 fs). Ultrafast dynamics are inferred by comparison to theory based on *ab initio* potential-energy calculations for the initial, intermediate, and final states and simulated sub-femtosecond wave packet propagation along the potential curves (Fig. 1). This atomic-clock scheme is particularly well suited to fragmentation of hydrogen halides, in which the hydrogen atom carries almost all of the released kinetic energy [14]. Our results show RXS spectra obtained from deep-core-hole excitation of HCl are sensitive to the nuclear motion of only a few picometers. Sensitivity to picometer nuclear motion identifies RXS as a potential method to study

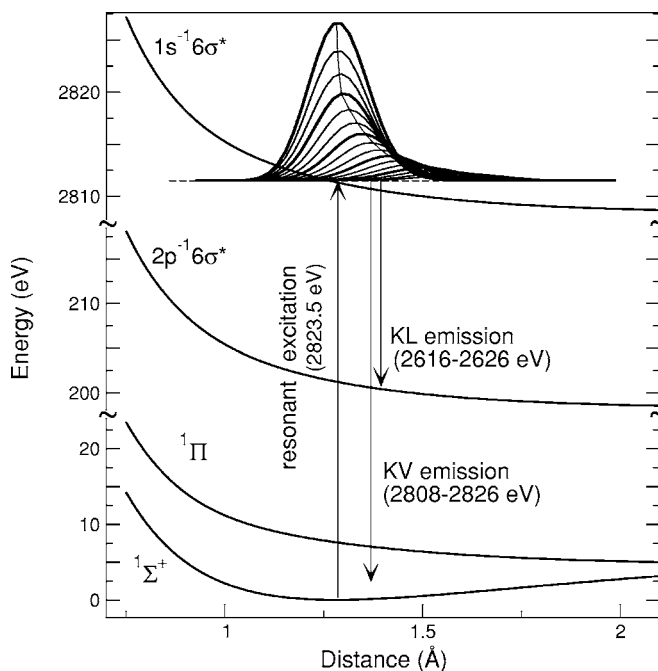


FIG. 1. Calculated potential energy surfaces of HCl (see text) and the square of the wave packet at different times separated by 0.2 fs.

*Corresponding authors. E-mail address: marc.simon@ccr.jussieu.fr

†On leave from IA&E SORAN.

dynamical effects in a wide variety of systems. Because ultrafast dissociation is not required to achieve such small changes in bond lengths, any nondissociating system with a deep-core level is amenable to study.

HCl has been chosen because it is a simple system that allows a thorough numerical investigation, and at the same time fully displays the physical mechanisms of this study. It serves also as a prototype of chlorine containing compounds like freons, which play an important role in physical-chemical properties of the ozone layer of atmosphere. All of these molecules are unstable or weakly bound in the first core-excited state because the core-excited chlorine atom is equivalent to an argon atom. This is confirmed by our recent experimental and theoretical investigations on freons [15].

The key to extracting ultrafast temporal dynamics from RXS measurements is high spectral resolution, which is limited by both physical and instrumental factors. Continuous experimental advances have improved the spectral resolution of both soft-x-ray [6] and hard-x-ray [16] spectrometers, leaving two physical limitations, lifetime and vibrational broadening, as major factors. RXS is a well-known technique to overcome lifetime broadening [17,18]. Furthermore, vibrational broadening in RXS is quenched in two cases: (i) if the potential surfaces for the ground and final states are the same (quenching away from resonance); or (ii) if the potential surfaces for the core-excited and final states are the same (quenching on the top of resonance) [19]. We demonstrate experimentally that complete quenching of vibrational broadening is a general phenomenon in RXS contrary to resonant Auger scattering where such effect is accidental [5,20].

The experiments were performed on beamline 9.3.1 at the Advanced Light Source (Lawrence Berkeley National Laboratory), which includes a Si(111) double-crystal monochromator with a resolution of approximately 0.4 eV for nearly 100% linearly polarized x-rays near the dissociative Cl $1s \rightarrow 6\sigma^*$ resonance (2822–2826 eV). Molecular x-ray emission (RXS) was measured using a new spectrometer based on a similar instrument [16]. Briefly, the HCl target is isolated in a static gas cell, separated from a beamline vacuum by 0.2 μm Si₃N₄ windows, at pressures between 250 and 440 Torr to minimize reabsorption of the emitted radiation. X-rays emitted vertically normal to the horizontal incident x-ray beam are dispersed in the plane parallel to the incident beam by a Si(111) curved-crystal spectrometer and detected by a resistive-anode, position-sensitive detector.

The incident radiation has a full width at half maximum (FWHM) of 0.5 eV, and the spectrometer broadening is 0.6 eV FWHM; total instrumental broadening is approximately 0.8 eV FWHM. The lifetime width of a Cl K hole Γ is 0.64 eV FWHM (Ref. 21). Measurements of Cl K - L emission (also called $K\alpha$ and corresponding to $1s^{-1} \rightarrow 2p^{-1}$ transitions, 2616–2630 eV) are shown in Fig. 2, where they exhibit the characteristic spin-orbit doublet. The Cl K - V emission (Fig. 3), also called $K\beta$, results from inelastic transitions to $^1\Sigma$ (~ 2811 eV) and $^1\Pi$ (~ 2815 eV) single valence hole final states, as well as elastic scattering. For both Cl K - L and K - V emission, the spectral shape depends strongly on excitation photon energy, ω , near the maximum of the Cl $1s \rightarrow 6\sigma^*$ resonance, where $\Omega = \omega - \omega_0$ is the detuning of ω

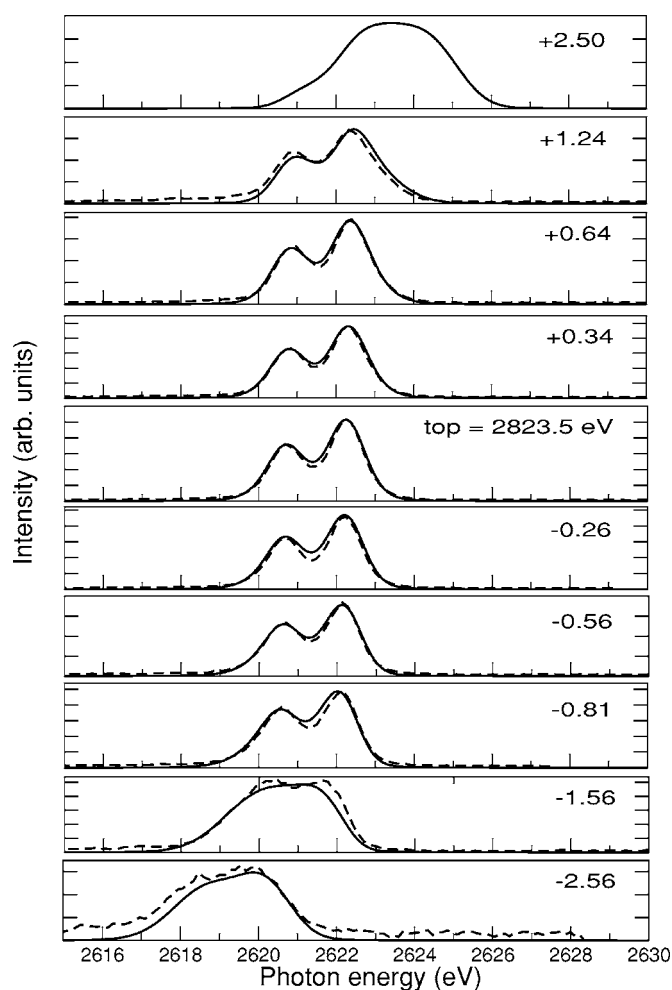


FIG. 2. Experimental (dots) and theoretical (curves) K - L emission spectra for various detunings Ω of the incident photon energy from the maximum of the $1s \rightarrow 6\sigma^*$ transition. The simulations used the experimental spin-orbit splitting (≈ 1.56 eV) and intensity ratio at the top of the absorption resonance (≈ 1.49).

from the frequency of the vertical x-ray absorption transition, ω_0 .

Theoretical simulations are based on a wave-packet theory [5,22,23], yielding cross sections for RXS of monochromatic radiation by randomly oriented molecules. All potentials were computed using density functional theory, with the hybrid function Becke three-parameter hybrid combined with Lee-Yang-Parr correlation functional (B3LYP) and the basis sets IGLO-III for chlorine and a correlation-consistent basis set of quintuple zeta quality (cc-pV5Z) for hydrogen. Because the K and L core holes are effectively the same with respect to interatomic interactions, the dissociative potentials of the core-excited and final states are almost parallel (see Fig. 1). Alternative and interesting wave packet approaches were developed in Refs. [24,25].

K - L emission. It is known that the duration time τ of RXS is drastically reduced by frequency detuning [4,5], i.e., adjusting the excitation energy away from the top of the resonance results in interference suppression of large-time contributions to the scattering process. In the Kramers-Heisenberg formula [5,23] for RXS, the Franck-Condon

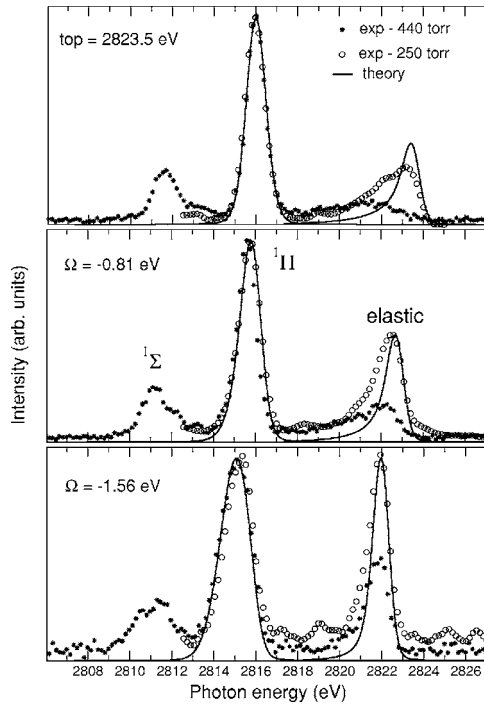


FIG. 3. HCl Cl K - V experimental (250 Torr, dots; 440 Torr, circles) and theoretical (curves) spectra.

(FC) factors between the parallel potentials of the core-excited $1s$ -hole state and the final $2p$ -hole state reduce to a Dirac function [case (ii) for vibrational quenching]. In this case, the RXS cross section $\sigma_0(\omega, \omega_1)$ can be written in a time-independent form as a product of a bound-free FC factor and a Lorentzian function accounting for the lifetime Γ ,

$$\sigma_0(\omega, \omega_1) \propto \frac{F(\Omega_1 - \Omega)}{\Omega_1^2 + \Gamma^2/4}. \quad (1)$$

Here $F(\Omega_1 - \Omega) \propto \exp\{-[(\Omega_1 - \Omega)/\Delta]^2 \ln 2\}$, where $\Omega_1 = \omega_1 - \omega_{cf}(\infty)$ and $\omega_{cf}(\infty)$ is the resonant frequency of the K - L transition in an isolated Cl atom. The proportionality factor in Eq. (1) stands for electronic matrix elements, and $\Delta \approx 1.68$ eV is the FWHM of the FC factor [23]. Equation (1) explains the broadening of the RXS profile for large detuning; dynamical broadening caused by the FC distribution is quenched on top of the photoabsorption resonance, $\Omega=0$, where the width of the K - L line approaches Γ . Such a collapse effect is clearly seen in the experimental spectra of Fig. 2. Experimental and theoretical dispersions and widths are shown in Fig. 4, where the width of one K - L line is plotted as a function of excitation energy. The physical reason for the collapse of the K - L lines is that the decay transitions occur between inner shells, $2p$ and $1s$, which have parallel potential surfaces. This makes the collapse (as well as for any inner shell transitions) a general phenomenon in contrast to resonant Auger scattering from molecules [20] where the potentials of the core-excited and final states are by coincidence parallel. This is one of the main results of our study.

The short lifetime of Cl K shell results in a nonlinear dispersion of K - L lines [Fig. 4(a)], which drastically differs from a conventional nondispersive dissociative peak in a soft-x-ray region [8–12]. It happens because the widths of the bound-free FC factor and the Lorentzian term in Eq. (1) are comparable in hard x rays.

K - V emission $^1\Pi$ band. The potential of the $^1\Pi$ final state is nearly parallel to the core-excited-state potential. Thus, the

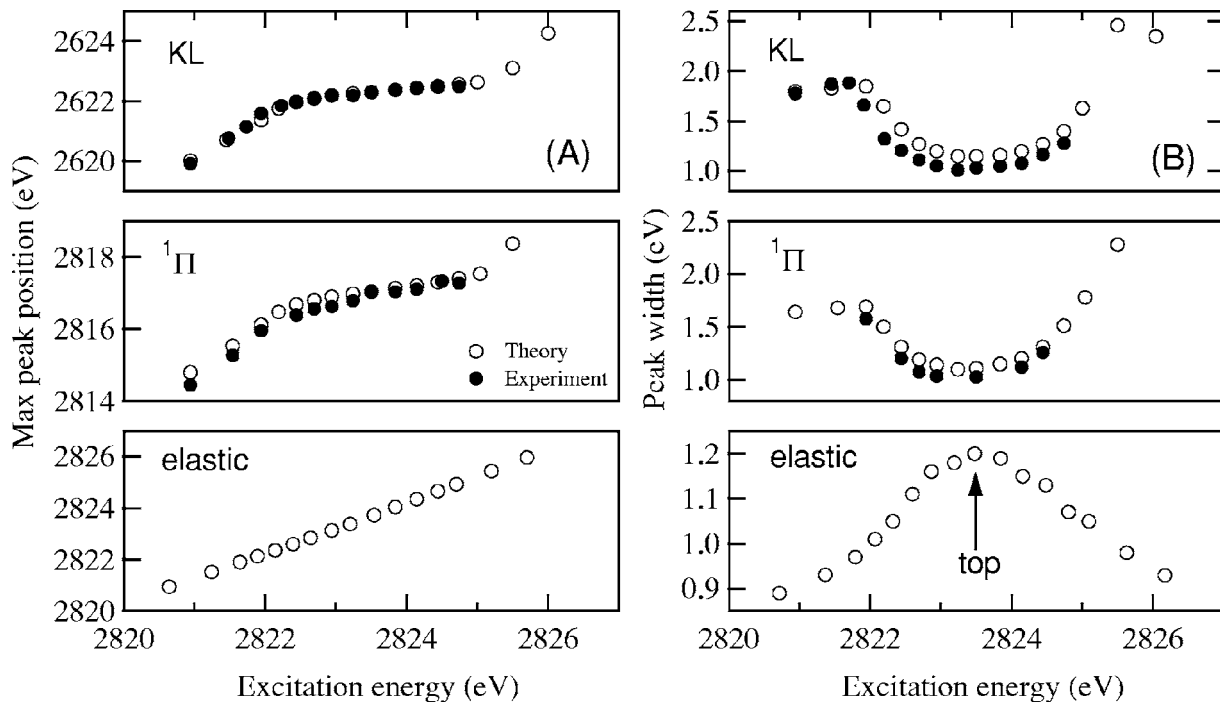


FIG. 4. (a) Dispersion. (b) Spectral widths (FWHM). Emitted photon frequency is taken at the maximum peak position.

behaviors of the $^1\Pi$ band and the K - L lines are very similar, as seen in Fig. 4.

Elastic band. For elastic scattering, the final electronic state is the ground state [case (i) for vibrational quenching is strictly valid here contrary to resonant Auger scattering]. When the detuning is large, the duration of the scattering [5] $\tau = (4\Omega^2 + \Gamma^2)^{-1/2}$ is short, and the wave packet does not have time to spread on the core-excited potential surface. This results in a general effect: the collapse of the vibrational structure of the elastic band [5,19] (Fig. 3), with a width equal to the instrumental broadening. It is worth noting that far away below the photoabsorption resonance, Thomson scattering is the major contribution to the elastic scattering [5]. Deviation of the simulated shapes of the elastic band relative to experiment is due to the reabsorption of emitted radiation, shown by the pressure dependence of the experimental spectra.

To summarize, femtosecond-scale nuclear dynamics have been observed using resonant x-ray Raman scattering in the hard-x-ray region. The results show RXS spectra obtained from deep-core shell excitation are sensitive to the nuclear motion of a few picometers, yielding information about the potential surfaces of the ground, core-excited, and final molecular states by comparing experimental results with simu-

lated RXS spectra. It was demonstrated, experimentally and theoretically, that RXS produces spectral lines without vibrational broadening. This is because the conditions for both types of vibrational collapse (parallelism of ground and final, or core-excited and final states) are naturally fulfilled in resonant x-ray Raman scattering, in contrast to resonant Auger electron scattering. This narrowing of RXS bands is thus predicted to be a general phenomenon. The short lifetime of the core-excited state in the hard-x-ray region leads to a complete breakdown of the conventional nondispersive behavior of soft-x-ray transitions between parallel potential surfaces. Finally, the sensitivity to picometer nuclear motion indicates RXS can probe dynamical effects in virtually any system with a deep-core level, because ultrafast dissociation is *not* required to achieve such small changes in bond lengths.

We acknowledge the financial support of PICS by the CNRS. Support from the National Science Foundation under NSF (Grant No. PHY-01-40375) is gratefully acknowledged. The authors also thank the staff of the ALS for their excellent support, especially Ed Wong. The ALS is supported by the U.S. DOE (Contract No. DE-AC03-76SF00098). This work was also supported by the Swedish Research Council (V.R.) and by the STINT Foundation.

-
- [1] C. Bressler and M. Chergui, *Chem. Rev.* (Washington, D.C.) **104**, 1781 (2004).
 [2] M. Drescher *et al.*, *Nature* (London) **419**, 803 (2002).
 [3] M. Drescher *et al.*, *Z. Phys. Chem.* **218**, 1147 (2004).
 [4] F. Gel'mukhanov, P. Salek, T. Privalov, and H. Ågren, *Phys. Rev. A* **59**, 380 (1999).
 [5] F. Gel'mukhanov and H. Ågren, *Phys. Rep.* **312**, 87 (1999).
 [6] S. L. Sorensen and S. Svensson, *J. Electron Spectrosc. Relat. Phenom.* **114–116**, 1 (2001).
 [7] K. Ueda, *J. Phys. B* **36**, R1-R47 (2003).
 [8] P. Morin and I. Nenner, *Phys. Rev. Lett.* **56**, 1913 (1986).
 [9] O. Björneholm *et al.*, *Phys. Rev. Lett.* **84**, 2826 (2000).
 [10] M. Neeb *et al.*, *Phys. Rev. Lett.* **76**, 2250 (1996).
 [11] I. Hjelte *et al.*, *Chem. Phys. Lett.* **334**, 151 (2001).
 [12] M. Kitajima *et al.*, *Phys. Rev. Lett.* **91**, 213003 (2003).
 [13] M. Magnuson *et al.*, *Phys. Rev. A* **59**, 4281 (1999).
 [14] D. L. Hansen *et al.*, *Phys. Rev. A* **58**, 3757 (1998).
 [15] A. Hudson *et al.*, (to be published).
 [16] S. Brennan *et al.*, *Rev. Sci. Instrum.* **60**, 2243 (1989).
 [17] P. Eisenberger *et al.*, *Phys. Rev. Lett.* **36**, 623 (1976).
 [18] S. Aksela, E. Kukkk, H. Aksela, and S. Svensson, *Phys. Rev. Lett.* **74**, 2917 (1995).
 [19] F. Gel'mukhanov, T. Privalov, and H. Ågren, *Phys. Rev. A* **56**, 256 (1997).
 [20] S. Sundin *et al.*, *Phys. Rev. Lett.* **79**, 1451 (1997).
 [21] J. A. Campbell, *At. Data Nucl. Data Tables* **77**, 1 (2001).
 [22] F. Gel'mukhanov and H. Ågren, *Phys. Rev. A* **54**, 379 (1996).
 [23] P. Sałek, F. Gel'mukhanov, and H. Ågren, *Phys. Rev. A* **59**, 1147 (1999).
 [24] Z. W. Gortel and D. Menzel, *Phys. Rev. A* **58**, 3699 (1998).
 [25] E. Pahl, L. S. Cederbaum, H. D. Meyer, and F. Tarantelli, *Phys. Rev. Lett.* **80**, 1865 (1998).